DOI 10.1007/s10778-015-0694-6
International Applied Mechanics, Vol. 51, No. 3, May, 2015

SATURATION OF ALMOST PERIODIC AND CHAOTIC AEROELASTIC OSCILLATIONS OF PLATES UNDER A RESONANT MULTIMODE FORCE

K. V. Avramov and E. A. Strel'nikova

A new approach based on the solution of a singular integral equation to analyzing the aeroelastic oscillations of thin plates is proposed. The velocity circulation is expanded into a series in the generalized coordinates of oscillations of the plate. This allows using a system with a finite number of degrees of freedom for the generalized coordinates to describe the aeroelastic oscillations. The following scenario is analyzed: the motion of the plate undergoes Neimark bifurcations and transform into quasiperiodic oscillations, which, in turn, transform into chaotic oscillations

Keywords: aeroelastic nonlinear oscillations, potential flow, incompressible nonviscous fluid, thin plate, generalized coordinates of oscillations of plate, Neimark bifurcation, quasiperiodic oscillations, chaotic oscillations

1. Introduction. The dynamics of thin-walled structures in a gas flow has attracted the close attention of scientists and engineers for more than half a century. This problem is extremely important in the fields of space engineering, power engineering, and transport. The fundamentals of aerofoil dynamics are outlined in [2–4]. To determine the distributed pressure forces acting on a vibrating plate, hypersingular integral equations are used. The theory of these equations and numerical methods for solving them are discussed in [6, 11–13]. The stability of aeroelastic oscillations of plates in a gas flow is analyzed in [7, 14]. The flutter of plates in a gas flow is studied in [15, 16]. The chaotic oscillations of a plate in a flow are addressed in [5]. The interaction of cylindrical shells with a gas flow is studied in [9]. Traveling waves in cylindrical shells interacting with a fluid are discussed in [10].

Here we propose a new method for analyzing the aeroelastic oscillations of plates undergoing geometrically nonlinear deformation. To determine the circulation density, we will solve a hypersingular integral equation. The velocity circulation will be expanded into a series in the generalized coordinates of flexural oscillations of the plate.

The set of circulation density functions does not depend on time and is determined only once during the solution of the problem. The effectiveness of this method is in using a nonlinear system with a finite number of degrees of freedom for the generalized coordinates of flexural oscillations of the plate. This dynamic system of low dimension can be analyzed in detail.

2. Problem Formulation and Basic Equations. Consider a cantilevered thin rectangular plate (Fig. 1). Since it is thin, its shear and rotary inertia can be neglected. The stresses and strains of the plate are related by Hooke's law. When a gas flow is past a thin plate on both its sides (Fig. 1), flutter (self-sustained oscillations) occurs. These unstable oscillations of the plate are constrained by the forces due to geometrically nonlinear deformation. Then the displacements of the plate are commensurable with its thickness. Such deformation of the plate is described by the von Kármán equations

$$\frac{h^2}{12}\nabla^4 w+\frac{1-\nu^2}{E}(\rho\ddot{w}+c\dot{w})-w_{xx}\left(u_x+\nu v_y+\frac{1}{2}w_x^2+\frac{\nu}{2}w_y^2\right)-(1-\nu)w_{xy}\left(u_y+v_x+w_x w_y\right)$$

A. N. Podgorny Institute for Mechanical Engineering Problems, National Academy of Sciences of Ukraine, 2/10 Dm. Pozharskogo St., Kharkiv, Ukraine 61046, e-mail: kvavr@kharkov.ua. Translated from Prikladnaya Mekhanika, Vol. 51, No. 3, pp. 113–121, May–June 2015. Original article submitted December 21, 2011.

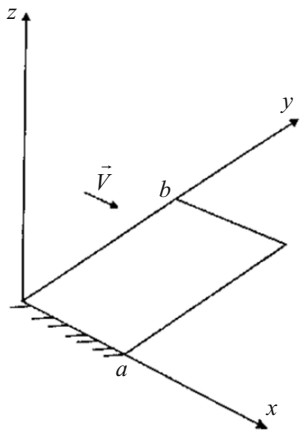

Fig. 1

$$-w_{yy}\left(v_y+\nu u_x+\frac{1}{2}w_y^2+\frac{\nu}{2}w_x^2\right)+\frac{1-\nu^2}{Eh}\left[p|_{z=+0}-p|_{z=-0}\right]=0, \tag{1}$$

$$u_{xx}+\frac{1-\nu}{2}u_{yy}+\frac{1+\nu}{2}v_{xy}-\frac{1-\nu^2}{E}\rho\ddot{u}+\frac{1+\nu}{2}w_{xy}w_y+w_xw_{xx}+\frac{1-\nu}{2}w_xw_{yy}=0, \tag{2}$$

$$v_{yy}+\frac{1-\nu}{2}v_{xx}+\frac{1+\nu}{2}u_{xy}-\frac{1-\nu^2}{E}\rho\ddot{v}+\frac{1+\nu}{2}w_{xy}w_x+w_yw_{yy}+\frac{1-\nu}{2}w_yw_{xx}=0, \tag{3}$$

where $u(x, y, t), v(x, y, t), w(x, y, t)$ are the displacements of particles of the plate's midsurface along the coordinate axes; ρ is the density of the plate; E and ν are the elastic modulus and Poisson's ratio; h is the thickness of the plate; $p|_{z=+0}$ and $p|_{z=-0}$ are the pressures on the upper and lower faces of the plate.

The plate occupies the domain $\Lambda=\{(x, y)\in[0, a]\times[0, b]\}$. The boundary conditions for the plate are

$$w|_{y=0}=\left.\frac{\partial w}{\partial y}\right|_{y=0}=v|_{y=0}=u|_{y=0}=0,$$

$$\left[Q_y+\frac{\partial M_{xy}}{\partial x}\right]_{y=b}=M_y|_{y=b}=N_y|_{y=b}=N_{xy}|_{y=b}=0,$$

$$Q_x+\frac{\partial M_{xy}}{\partial y}=M_x=N_x=N_{xy}=0,\quad x=0, a, \tag{4}$$

where N_x, N_y, N_{xy} are the membrane forces in the mid-surface of the plate; Q_x and Q_y are the transverse forces; M_x, M_y, M_{xy} are the bending and twisting moments in the plate.

The gas past the vibrating plate is assumed nonviscous, incompressible, three-dimensional, and nonstationary, and far from the plate, its velocity $\vec{V}$ is constant and parallel to the x-axis.

The oscillations of the plate cause three-dimensional nonstationary perturbation of the gas flow near the plate. This perturbation is described by a velocity vector $\vec{U}$ with components $\widetilde{U}(x, y, z, t), \widetilde{V}(x, y, z, t), \widetilde{W}(x, y, z, t)$. Assume that the motion of the fluid is irrotational. Then there exists a velocity potential $\varphi(x, y, z, t)$ defined as $\vec{U}=\vec{V}+\nabla\varphi$. The function $\varphi(x, y, z, t)$ satisfies the Laplace equation. Consider the boundary conditions that this equation must satisfy. One is no flow through the plate:

$$\left.\frac{\partial\varphi}{\partial z}\right|_{z=\pm0}=V\frac{\partial w}{\partial x}+\frac{\partial w}{\partial t}, \tag{5}$$

where $z = \pm 0$ denote the upper and lower faces of the plate.

The pressure on the plate can be determined from Bernoulli's equation:

$$\frac{1}{\rho_w}\left[p|_{z=w+0} - p|_{z=w-0}\right] = \frac{\partial}{\partial t}\left[\varphi|_{z=w-0} - \varphi|_{z=w+0}\right] + V\frac{\partial}{\partial x}\left[\varphi|_{z=w-0} - \varphi|_{z=w+0}\right] = \frac{\partial \gamma}{\partial t} + V\frac{\partial \gamma}{\partial x}, \tag{6}$$

where $\gamma = \varphi|_{z=w-0} - \varphi|_{z=w+0}$ is the circulation density; $\varphi|_{z=w+0}$ and $\varphi|_{z=w-0}$ are the values of the velocity circulation on the upper and lower faces of the plate.

The solution of the Laplace equation can be represented as a double-layer potential:

$$\varphi(x, y, z, t) = \frac{1}{4\pi}\int_{\Lambda} \gamma(\xi, t)\frac{\partial}{\partial n_\xi}\frac{1}{\sqrt{(x-\xi_1)^2 + (y-\xi_2)^2 + (z-\xi_3)^2}}\, d\xi_1 d\xi_2 d\xi_3, \tag{7}$$

where n_ξ is the unit normal vector to the surface of the plate.

Substituting Eq. (7) into Eq. (5), we obtain a hypersingular integral equation for the circulation density γ:

$$V\frac{\partial w}{\partial x} + \frac{\partial w}{\partial t} = \frac{1}{4\pi}\int_{\Lambda} \frac{\gamma(\xi_1, \xi_2, t)\, d\xi_1 d\xi_2}{\left[(x-\xi_1)^2 + (y-\xi_2)^2\right]^{3/2}}. \tag{8}$$

Let us expand the amplitude of the self-sustained oscillations of the plate into a series of its natural modes:

$$w = \sum_{j=1}^{N_1} q_j(t)\psi_j(x, y),$$

$$u = \sum_{j=1}^{N_2} l_j(t)\tilde{\varphi}_j(x, y),$$

$$v = \sum_{j=1}^{N_3} \eta_j(t)\tilde{\theta}_j(x, y), \tag{9}$$

where $q_j(t), l_j(t), \eta_j(t)$ are the generalized coordinates of the plate; $\psi_j(x, y), \tilde{\varphi}_j(x, y), \tilde{\theta}_j(x, y)$ are the natural modes of its linear oscillations.

Let us express the velocity circulation density in terms of aerodynamic derivatives:

$$\gamma(\xi_1, \xi_2, t) = \sum_{j=1}^{N_1}\left[V q_j(t)\Delta_j(\xi_1, \xi_2) + \dot{q}_j(t)\tilde{\delta}_j(\xi_1, \xi_2)\right], \tag{10}$$

where $\Delta_j, \tilde{\delta}_j$ are unknown functions.

Substituting (9) and (10) into the hypersingular integral equation (8), we get a system of hypersingular integral equations for $\Delta_j, \tilde{\delta}_j$:

$$\frac{\partial \psi_j}{\partial x} = \frac{1}{4\pi}\int_S \frac{\Delta_j(\xi_1, \xi_2)\, d\xi_1 d\xi_2}{\left[(x-\xi_1)^2 + (y-\xi_2)^2\right]^{3/2}},$$

$$\psi_j = \frac{1}{4\pi}\int_S \frac{\tilde{\delta}_j(\xi_1, \xi_2)\, d\xi_1 d\xi_2}{\left[(x-\xi_1)^2 + (y-\xi_2)^2\right]^{3/2}},$$

$$j = 1, \ldots, N_1. \tag{11}$$

Let us now nondimensionalize system (11):

$$\xi = xa^{-1}, \quad \eta = yb^{-1}, \quad \overline{\xi}_1 = \xi_1 a^{-1}, \quad \overline{\xi}_2 = \xi_2 b^{-1}, \quad \chi_* = b^2 a^{-2}, \quad \overline{\Delta}_j = \widetilde{\delta}_j a^{-1}.$$

The solutions of the hypersingular integral equations (11) can be found with the numerical method proposed in [2, 3]. This method reduces the system of hypersingular integral equations to a system of linear algebraic equations.

3. Method for the Analysis of Nonlinear Oscillations. Let us use a model with a finite number of degrees of freedom to describe the oscillations of the plate. Substituting series (9) into Eqs. (2) and (3), discarding the inertial terms (which is possible because the plate is thin and the natural frequencies of longitudinal oscillations are much higher than those of bending oscillations), and applying the Galerkin method, we obtain a system of linear algebraic equations for $(l_1, \ldots, l_N, \eta_1, \ldots, \eta_N)$:

$$\sum_{\mu=1}^{N}\left[\gamma_{j\mu}^{(1,1)} l_\mu + \gamma_{j\mu}^{(1,2)} \eta_\mu\right] = -\sum_{i=1}^{N_1}\sum_{\mu=1}^{N_1} R_{ji\mu}^{(1)} q_i q_\mu,$$

$$\sum_{\mu=1}^{N}\left[\gamma_{j\mu}^{(2,1)} l_\mu + \gamma_{j\mu}^{(2,2)} \eta_\mu\right] = -\sum_{i=1}^{N_1}\sum_{\mu=1}^{N_1} R_{ji\mu}^{(2)} q_i q_\mu, \quad j = 1, \ldots, N, \tag{12}$$

where the parameters $\gamma_{j\mu}^{(1,1)}, \ldots, \gamma_{j\mu}^{(2,2)}, R_{ji\mu}^{(1)}, R_{ji\mu}^{(2)}$ are determined as double integrals of basis functions.

These formulas are omitted for brevity. The inverse matrix of the system of linear algebraic equations (12) is denoted as $r = \{r_{ij}\}_{j=1,\ldots,2N}^{i=1,\ldots,2N}$. Then the solution of the system of linear algebraic equations is represented as

$$l_k = \sum_{i=1}^{N_1}\sum_{\mu=1}^{N_1} \delta_{ki\mu} q_i q_\mu, \quad \eta_k = \sum_{i=1}^{N_1}\sum_{\mu=1}^{N_1} \delta_{N+k,i\mu} q_i q_\mu \quad (k = 1, \ldots, N) \tag{13}$$

$$\left[\delta_{ki\mu} = -\sum_{p=1}^{N}\left(r_{kp} R_{\pi\mu}^{(1)} + r_{k,\,N+p} R_{\pi\mu}^{(2)}\right);\ k = 1, \ldots, 2N;\ i = 1, \ldots, N_1;\ \mu = 1, \ldots, N_1\right].$$

Substituting (13) into (9), the result into Eq. (1), and using the Bubnov–Galerkin method, we get a dynamic system with a finite number of degrees of freedom for the following dimensionless variables and parameters:

$$\vartheta_j = \frac{q_j}{h}, \quad j = 1, \ldots, N_1, \quad \tau = p_1 t, \quad \alpha = \frac{c}{\rho\, p_1}, \quad \Omega_j = \frac{p_j}{p_1}. \tag{14}$$

Doing so gives an autonomous system of ordinary differential equations describing the oscillations of the plate:

$$\sum_{i=1}^{N_1}\left(m_{ji}\vartheta_i'' + \alpha\widetilde{\delta}_{ji}\vartheta_i' + \Omega_i^2 k_{ji}\vartheta_i\right) = \sum_{p=1}^{N_1}\sum_{i=1}^{N_1}\sum_{\mu=1}^{N_1} f_{jpi\mu}\vartheta_p\vartheta_i\vartheta_\mu, \quad j = 1, \ldots, N_1. \tag{15}$$

The elements of the matrices of the linear part of this system are expressed so as to obtain explicit dependence on the Mach number M:

$$m_{ji} = \Theta_{ji} + \lambda\int_{\overline{S}} \overline{\Delta}_i \psi_j\, d\overline{\xi}_1 d\overline{\xi}_2, \quad k_{ji} = \Theta_{ji} + M^2\varepsilon_{ji}, \quad \widetilde{\delta}_{ji} = \Theta_{ji} + M\varphi_{ji}.$$

To apply the describing function method to the analysis of the self-sustained oscillations in system (15), we represent its motion as

$$\vartheta_i = A_i \cos(\omega t) + B_i \sin(\omega t), \tag{16}$$

where ω is the unknown frequency.

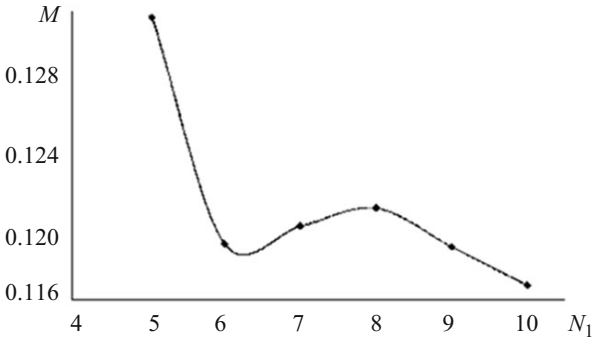

Fig. 2

System (15) is autonomous; therefore, it is invariant under change of variables $t \to t + t_0$, where t_0 is an arbitrary constant. The parameter t_0 is selected so that $A_1 \equiv 0$. Following the describing function method, we determine the amplitudes of harmonics $A_2, A_3, \ldots, A_{N_1}, B_1, \ldots, B_{N_1}$ (16) from the following system of nonlinear algebraic equations:

$$\sum_{i=1}^{N_1} \left\{ \left[\Omega_i^2 \left(\Theta_{ji} + M^2 \varepsilon_{ji} \right) - m_{ji} \omega^2 \right] A_i + \alpha \left(\Theta_{ji} + M \varphi_{ji} \right) \omega B_i \right\} = \sum_{p=1}^{N_1} \sum_{i=1}^{N_1} \sum_{\mu=1}^{N_1} f_{jpi\mu} F_{\pi\mu}^{(c)},$$

$$\sum_{i=1}^{N_1} \left\{ \left[\Omega_i^2 \left(\Theta_{ji} + M^2 \varepsilon_{ji} \right) - m_{ji} \omega^2 \right] B_i - \alpha \left(\Theta_{ji} + M \varphi_{ji} \right) \omega A_i \right\} = \sum_{p=1}^{N_1} \sum_{i=1}^{N_1} \sum_{\mu=1}^{N_1} f_{jpi\mu} F_{\pi\mu}^{(s)},$$

$$j = 1, \ldots, N_1,$$

$$4F_{\pi\mu}^{(c)} = 3A_p A_i A_\mu + A_p B_i B_\mu + B_p A_i B_\mu + B_p B_i A_\mu,$$

$$4F_{\pi\mu}^{(s)} = 3B_p B_i B_\mu + A_p A_i B_\mu + A_p B_i A_\mu + B_p A_i A_\mu. \qquad (17)$$

System (17) is analyzed numerically using the continuation algorithm detailed in [1].

4. Numerical Analysis of Oscillations. Let us numerically analyze the oscillations of the cantilevered plate shown in Fig. 1. To determine the natural modes used in (9), we apply the Rayleigh–Ritz method. Consider the aeroelastic oscillations of a plate with parameters used in [17]: $a = b = 0.3$ m, $h = 0.001$ m, $E = 0.69 \cdot 10^{11}$ Pa, $\nu = 0.3$, $\rho = 2.3 \cdot 10^3$ kg/m^3.

Note that the fifth and sixth natural frequencies of the plate satisfy the condition of internal resonance 1:1:

$$\Omega_5 = \Omega_6 + \varepsilon\sigma, \qquad (18)$$

where $\varepsilon << 1$, σ is the mismatch parameter.

Let us determine the number of degrees of freedom needed to predict the Mach number M at which flutter occurs. For different number of degrees of freedom of the system, we will determine the Mach number at which Hopf bifurcation occurs. Let the linear damping factor of the plate $\alpha = 0.006$. The calculated results are shown in Fig. 2. Hopf bifurcation does not occur at four degrees of freedom of the discrete model. It does at five degrees of freedom. Six degrees of freedom are sufficient to predict the velocity at which self-sustained oscillations occur.

The flow velocity V_H =42 m/sec at which flutter occurs was found in [17]. This value corresponds to the linear damping factor $\alpha = 0.006$. The flutter frequency ω_f = 90 rad/sec. The flutter frequency obtained in [17] ω_f = 84.85 rad/sec. Thus, our flutter predictions are in agreement with those in [17].

The convergence of model (15) was analyzed as well. To this end, the self-sustained oscillations in system (15) were analyzed for different number of basis functions in (9) using the describing function method. The number of modes in the series expansion of bending of the plate is fixed ($N_1 = 10$). The number of modes in the series expansion of longitudinal displacement was varied from 2 to 6. The calculated results are shown in Fig. 3. Hopf bifurcation occurs at the point H. The stable equilibrium state of the plate becomes unstable, and stable self-sustained oscillations occur (see Fig. 3). They correspond to the following

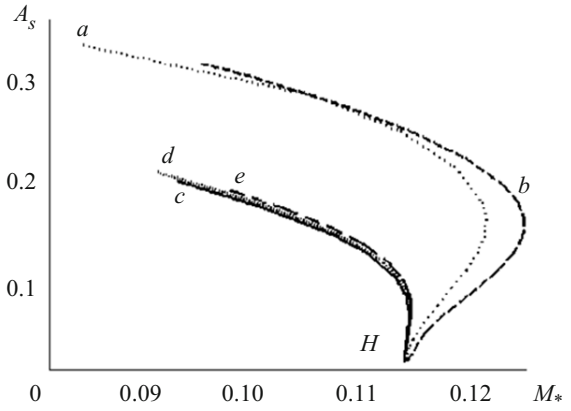

Fig. 3

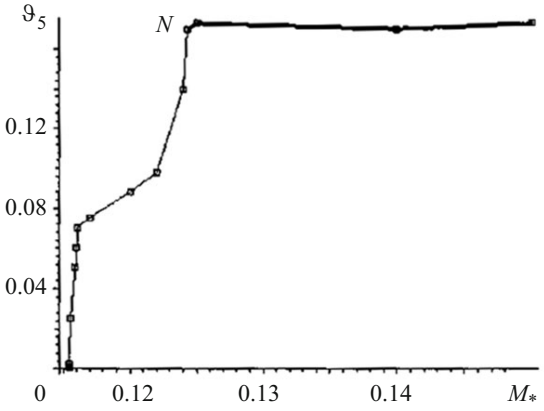

Fig. 4

parameters in series (9): $N = 2$ (curve *a*); $N = 3$ (curve *b*); $N = 4$ (curve *c*); $N = 5$ (curve *d*); $N = 6$ (curve *e*). Curves *c*, *d*, *e* are close, which suggests convergence of the results. Thus, $N = 4$ is sufficient to expand the displacement in the plate plane. For further calculations, we choose $N = 6$.

The results of direct numerical integration are presented in Fig. 4 which shows the amplitude of the generalized coordinate ϑ_5 as a function of the Mach number M_*. The thin solid line represents periodic oscillations. Neimark bifurcation occurs at the point *N* where the thin line connects with the heavy line. This bifurcation gives rise to almost periodic oscillations, which later become chaotic. The amplitude of such steady-state oscillations is shown in Fig. 4 by a heavy line. A long transient process occurs on the time interval $t \in [0; 2400(\pi/\omega_1)]$, where ω_1 is the flutter frequency, during almost periodic and chaotic oscillations.

If the integration is over the entire range of M_* in Fig. 4 rather than over the long time interval, then the oscillations look like steady-state periodic self-sustained.

To analyze almost periodic and chaotic oscillations, we calculated Poincarй's sections. To this end, we drew the plane $\Sigma = \{(\vartheta_1,\ldots,\vartheta_{10},\dot{\vartheta}_1,\ldots,\dot{\vartheta}_{10}) \in R^{20} \mid \dot{\vartheta}_5 = 0\}$ in the phase space of the system $(\vartheta_1,\ldots,\vartheta_{10},\dot{\vartheta}_1,\ldots,\dot{\vartheta}_{10})$ and determined the intersection of the phase path with this plane. The projection of the Poincaré sections of almost periodic oscillations onto the plane $(\vartheta_3,\dot{\vartheta}_3)$ immediately after the Neimark bifurcation $M_* = 0.125$ is shown in Fig. 5a.

There are 3000 points in this figure. The form of the Poincaré sections is indicative of an invariant torus in the system. As M_* is increased, almost periodic oscillations become chaotic. The projection of the Poincaré section Σ onto the plane $(\vartheta_6,\dot{\vartheta}_6)$ for $M = 0.14$ is shown in Fig. 5b, where 3000 points are plotted. Note that the oscillations are chaotic while $M < 0.18$. When $M_* = 0.18$, the oscillations go to infinity after a long transient $t \approx 2000\pi/\omega_1$.

Back on the analysis of the amplitudes in Fig. 4, we introduce a parameter $\tilde{\eta}$ describing the interaction between the generalized coordinates ϑ_5 and ϑ_6: $\tilde{\eta} = (\max(\vartheta_5))/(\max(\vartheta_6))$. As $\tilde{\eta}$ increases, the contribution of the generalized coordinate ϑ_5 increases; as $\tilde{\eta}$ decreases, the contribution of the generalized coordinate ϑ_6 increases.

Table 1 shows how the parameter $\tilde{\eta}$ depends on the number M_* for the steady-state oscillations represented in Fig. 4. If the oscillations are periodic, the contribution of the coordinate ϑ_5 is much greater. Figure 4 shows that the amplitude of periodic oscillations increases. After the Neimark bifurcation, however, the contribution of the generalized coordinate ϑ_6 increases considerably (see Table 1). A considerable amount of the oscillation energy of the generalized coordinate ϑ_5 is pumped over to the coordinate ϑ_6. This is why the amplitude of oscillations does not increase after the Neimark bifurcation. Note that the interaction between the generalized coordinates ϑ_5 and ϑ_6 is due to the internal resonance (17) between the natural frequencies. A similar phenomenon accompanying forced oscillations was described in [18]. This phenomenon is called saturation.

5. Conclusions. The self-sustained oscillations of a cantilevered square plate at internal resonance (1:1) between the fifth and sixth natural frequencies have been studied.

The modes corresponding to these frequencies interact during the self-sustained oscillations of the plate. The contribution of the generalized coordinate ϑ_5 to the periodic oscillations of the plate is much more significant than that of the coordinate ϑ_6.

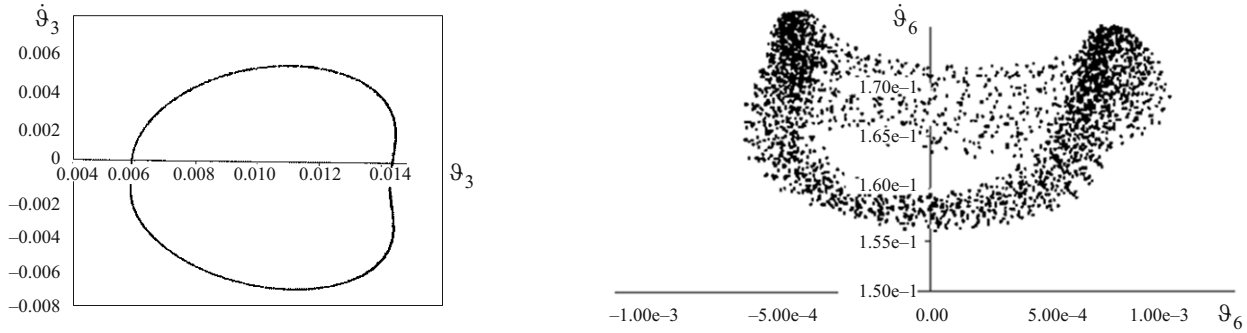

a *b*

Fig. 5

TABLE 1

M_*	0.115411	0.116078	0.124	0.125	0.14	0.15	0.17
$\tilde{\eta}$	3.324	3.25	3.09	2.8	2.43	2.43	1.93

The amplitude of these periodic oscillations sharply increases with increasing Mach number. After the Neimark bifurcation, the generalized coordinate ϑ_6 becomes much more active, and some amount of the oscillation energy of the generalized coordinate ϑ_5 is pumped over to the coordinate ϑ_6. As the number M increases, the amplitudes ϑ_5 of almost periodic and chaotic oscillations do not increase because their energy is pumped over to the generalized coordinate ϑ_6.

The model used predicts amplitudes that increase without limit with time. Certainly, the plate cannot undergo such a motion. In this case, the system displays more complicated motions, which are different from those studied here. To predict such a motion, it is necessary to keep nonlinear terms of higher order in modeling the geometrically nonlinear deformation of a plate.

REFERENCES

1. K. V. Avramov and Yu. V. Mikhlin, *Models*, *Methods*, *and Phenomena*, Vol. 1 of *Nonlinear Dynamics of Elastic Systems* [in Russian], Inst. Komp. Issled., Moscow–Izhevsk (2010).
2. S. M. Belotserkovskii, *Thin Lifting Surface in a Subsonic Gas Flow* [in Russian], Nauka, Moscow (1965).
3. N. F. Vorob'ev, *Aerodynamics of Lifting Surfaces in a Stationary Flow* [in Russian], Nauka, Novosibirsk (1985).
4. E. A. Krasil'shchikova, *A Thin Airfoil in a Compressible Flow* [in Russian], Nauka, Moscow (1978).
5. K. V. Avramov and E. A. Strel'nikova, "Chaotic oscillations of plates interacting on both sides with a fluid flow," *Int. Appl. Mech.*, **50**, No. 3, 303–309 (2014).
6. E. H. Dowell, H. C. Curtiss, R. H. Scanlan, and F. Sisto, *A Modern Course in Aeroelasticity*, Kluwer Academic Publishers, Dordrecht (1995).
7. C. Q. Guo and M. P. Paidoussis, "Stability of rectangular plates with free side-edges in two-dimensional inviscid channel flow," *ASME. J. Appl. Mech.*, No. 67, 171–176 (2000).
8. A. G. Haddow, A. D. S. Barr, and D. T. Mook, "Theoretical and experimental study of modal interaction in a two-degree-of-freedom structures," *J. Sound Vibr.*, **97**, 451–473 (1984).
9. P. S. Koval'chuk, L. A. Kruk, and V. A. Pelykh, "Stability of differently fixed composite cylindrical shells interacting with fluid flow," *Int. Appl. Mech.*, **50**, No. 6, 664–676 (2014).
10. V. D. Kubenko and P. S. Koval'chuk, "Modeling the nonlinear interaction of standing and traveling bending waves in fluid-filled cylindrical shells subject to internal resonances," *Int. Appl. Mech.*, **50**, No. 4, 353–364 (2014).

11. M. T. Landahl and V. J. E. Stark, “Numerical lifting-surface theory – problems and progress,” *AIAA J.*, No. 6, 2049–2060 (1968).
12. D. T. Mook and B. Dong, “Perspective: Numerical simulations of wakes and blade-vortex interaction,” *ASME. J. Fluids Eng.*, No. 116, 5–21 (1994).
13. L. Morino and C.-C. Kuo, “Subsonic potential aerodynamic for complex configurations: A general theory,” *AIAA J.*, No. 12, 191–197 (1974).
14. L. K. Shayo, “The stability of cantilever panels in uniform incompressible flow,” *J. Sound Vibr.*, No. 68, 341–350 (1980).
15. D. Tang, E. H. Dowell, and K. C. Hall, “Limit cycle oscillations of a cantilevered wing in low subsonic flow,” *AIAA J.*, No. 37, 364–371 (1999).
16. D. Tang and E. H. Dowell, “Limit cycle oscillations of two-dimensional panels in low subsonic flow,” *Int. J. Non-Lin. Mech.*, No. 37, 1199–1209 (2002).
17. D. Tang, E. H. Dowell, and K. C. Hall, “Limit cycle oscillations of a cantilevered wing in low subsonic flow,” *AIAA J.*, **37**, No. 3, 364–371 (1999).
18. Y. Watanabe, K. Isogai, S. Suzuki, and M. Sugihara, “A theoretical study of paper flutter,” *J. Fluids Struct.*, No. 16, 543–560 (2002).